

## Interband effect in the optical response of strontium clusters

C. Bréchnignac, Ph. Cahuzac, N. Kébaili, J. Leygnier, and H. Yoshida\*  
*Laboratoire Aimé Cotton CNRS II, Bâtiment 505, Campus d'Orsay, 91405 Orsay Cedex, France*  
 (Received 14 October 1999)

Photoabsorption spectroscopy has been performed on singly charged strontium clusters  $\text{Sr}_n^+$  for the sizes  $n=61, 127,$  and  $200,$  in the  $1.8$  to  $5.2$  eV energy range. Superimposed on the giant resonance, related to the Mie plasma resonance of a metallic sphere, the spectra reveal an extended wing in the high-energy range attributed to interband transitions. Evidence of striking correspondence with the absorption spectrum of a macroscopic sphere obtained from the measured real and imaginary parts of the bulk strontium dielectric function is shown.

Group II atoms have a closed-shell  $s^2$  electronic structure. With two  $s$  electrons per atom, these materials should in principle be insulators in the bulk. Their metallic character results from a hybridization, leading to a partially empty conduction band. The neutral dimers of group II atoms are weakly bound by van der Waals forces, leading to binding energy less than a few tenths of an eV [ $0.13$  eV for  $\text{Sr}_2$  (Ref. 1)] so that as cluster size increases a nonmetal-to-metal transition should occur. As has been shown for mercury clusters, such a transition is not sharp and the behavior of electronic properties such as optical absorption,<sup>2</sup> ionization potentials,<sup>3</sup> and photoemission spectroscopy<sup>4</sup> changes over a range of ten to a few hundred atom clusters. This behavior differs completely from that observed for alkali atom clusters, which exhibit a monotonic trend of their electronic properties against their size, making these species, having one  $s$  valence electron per atom, the prototype of metallic clusters.<sup>5</sup>

Little is known about alkaline-earth clusters. Most recent studies deal with the atomic geometry<sup>6</sup> and the most striking feature is an icosahedral close-packed structure for Mg, Ca, and Ba atom clusters.<sup>7,8</sup> We present here results for  $\text{Sr}_n^+$  clusters, probing their electronic structure by photoevaporation spectroscopy.<sup>5,9</sup> This method has been successfully applied to alkali atom, silver atom, and mercury atom clusters and has revealed the evolution of the collective excitation with size. In the case of bulk strontium the absorption spectrum presents an extended “blue” wing superimposed on the collective excitation of the conduction electrons, which is interpreted as an interband transition, implying a strong  $d$  electron effect and crystal structure.<sup>10</sup> So it is of fundamental interest to know if this electronic structure is also present for clusters and down to what cluster size such behavior can be observed.

The principle of the measurements is based on a combination of photoevaporation and mass spectroscopy achieved by a tandem time-of-flight device. The method that we have developed previously for alkali atom clusters has been described in detail in Ref. 9. It is especially appropriate for large-size clusters and leads to the determination of the absolute value of the absorption cross section  $\sigma^{\text{abs}}$  as a function of the photon energy.

A neutral distribution of clusters is generated by using a gas-aggregation source and photoionized by a uv laser pulse in the ionizing region of a time-of-flight mass spectrometer.

Ionized clusters first enter a field-free tube where they are mass selected by a pulsed electrostatic gate. Cluster ion bunches enter a decelerating-accelerating multiplate device where they interact with a second pulsed laser. The electronic excitation due to the photon absorption relaxes very rapidly among the vibrational modes, providing heating of the cluster. Evaporative cooling occurs during the residence time of the droplets within the interaction region (a few microseconds). The ion products are mass analyzed by a second time-of-flight mass spectrometer. However, the unimolecular evaporation time scale increases with cluster size, causing nondetectable dissociation during the observation time window after one-photon absorption. For measuring the absorption cross section of  $\text{Sr}_n^+$  in the  $60$ – $200$  atom cluster size range, multistep photon absorption is required, leading to a Poisson distribution of the ionic fragments. The absorption cross section  $\sigma^{\text{abs}}$  is deduced from the maximum of the fragment distribution, assuming that it varies very little with the number of absorbed photons. When only one evaporative channel is involved, corresponding to a dissociation energy  $D_n^+$ , the number of evaporations at the maximum intensity of the distribution is  $P_{\text{max}}$  such that

$$P_{\text{max}} = \alpha + \sigma^{\text{abs}} \phi \delta \frac{h\nu}{\langle D_n^+ \rangle}, \quad (1)$$

where  $\phi$ ,  $\delta$ , and  $h\nu$  are the photon flux, the laser pulse duration, and the photon energy, respectively.  $\langle D_n^+ \rangle$  is the average dissociation energy over the whole evaporative sequence, assumed to be a slowly varying function of the size.  $\alpha$  is a small dimensionless quantity determined by  $\langle D_n^+ \rangle$  and the time windows of the experiment.<sup>9</sup>

Figure 1 shows a typical mass spectrum of singly charged strontium clusters photoionized at  $5$  eV. One notices that small size clusters display predominant ion peak intensities at  $n=11, 19, 23, 34, 43, 52, 61,$  and  $81,$  which are also dominant in doubly charged species. This sequence differs from that observed in other alkaline-earth clusters.<sup>11</sup> In particular,  $n=13$  and  $55,$  characterizing the icosahedral compact structure, do not show large ion peak intensities. This is also in contradiction with recent calculations predicting icosahedral strontium cluster growth.<sup>8</sup> Moreover, this ion intensity pattern and especially the pronounced drop after  $n=61$  has been reported before for rare-earth clusters<sup>12</sup> and has not yet

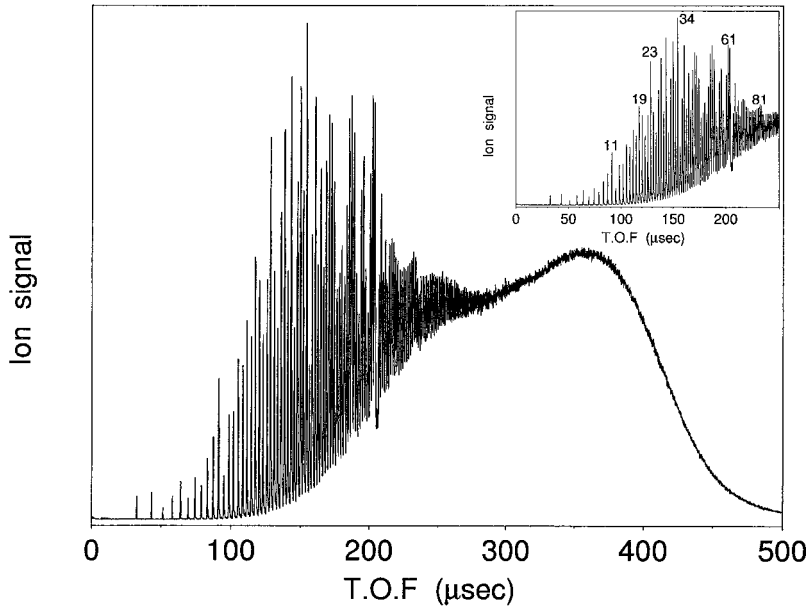


FIG. 1. Mass spectrum of  $\text{Sr}_n^+$  clusters photoionized at photon energy  $h\nu_i = 5$  eV.

been understood. In contrast with Eu and Yb rare-earth atom clusters, beyond  $\text{Sr}_{61}^+$  the intensities in the mass spectrum present a smooth behavior.

Figure 2 displays typical dissociation spectra of the  $\text{Sr}_{127}^+$  parent photoexcited at  $h\nu = 3.50$  eV for two different laser fluences. From the mass spectrum the maximum  $P_{\max}$  of the fragment distribution is obtained. Using Eq. (1) we can deduce the photoabsorption cross section  $\sigma^{\text{abs}}$  if we know the dissociation energy. For this purpose we have performed unimolecular decay and photodissociation experiments.<sup>13</sup> Strontium cluster dissociation proceeds via the evaporation of neutral monomers,  $\text{Sr}_n^+ \rightarrow \text{Sr}_{n-1}^+ + \text{Sr}$ . The dissociation energy varies little with size. In the range  $n = 7 - 100$  we found an average dissociation energy  $\langle D_{n,1}^+ \rangle \approx 1.2 \pm 0.1$  eV.

Figure 3 shows absorption cross section measurements for the cluster sizes  $n = 61, 127,$  and  $200$  in the  $1.81 - 5.20$  eV energy range. Photons are provided from the harmonics of a pulsed Nd-YAG (Yttrium Aluminum Garnet) laser associated with a hydrogen Raman shifter. The uncertainty of the data is essentially due to the determination of the laser fluence. It can be estimated to  $\pm 20\%$ . The behavior of the three cross sections is very similar, presenting a central core peaking at  $2.7$  eV with an extended “blue” wing. The absolute value of the absorption cross section at the maximum increases linearly with the cluster size.

As a first step, the central core of the profile, which is in the energy range of the plasma frequency, can be interpreted in terms of collective excitation of a metallic sphere. For spherical metallic particles, the radius of which is much smaller than the wavelength, the absorption cross section is

$$\sigma^{\text{abs}}(\omega) = \sigma^{\text{max}} \frac{\omega^2 \Gamma^2}{(\omega^2 - \omega_0^2)^2 + \omega^2 \Gamma^2}, \quad (2)$$

where  $\Gamma$  is the width of the resonance and  $\omega_0$  the frequency at its maximum. Fitting the central part of the experimental profiles with Eq. (2), one gets for all three sizes  $\hbar\omega_0 = 2.75 \pm 0.1$  eV, and  $\Gamma = 1.3 \pm 0.2$  eV. From the Drude model, the plasma frequency  $\omega_M$  of a metallic sphere is connected to its electron density  $n_e$ :

$$\hbar\omega_M = \hbar \sqrt{4\pi n_e e^2 / 3m_e}. \quad (3)$$

Equation (3) leads to  $\hbar\omega_M = 4.08$  eV for strontium, to be compared to the experimental quantity  $\hbar\omega_0 = 2.75$  eV, which then appears significantly redshifted for clusters in the size range studied. Such a redshift has also been found for alkali atom clusters as compared to the Drude plasma frequency,<sup>14</sup> due to the crudeness of the free-electron model.

To go further in the comparison between the photoexcitation of strontium clusters and the optical properties of the bulk, we synthesize the absorption cross section of a strontium macroscopic sphere from the measured optical constants,  $\epsilon(\omega)$ ,<sup>15</sup> by using the formula<sup>16</sup>

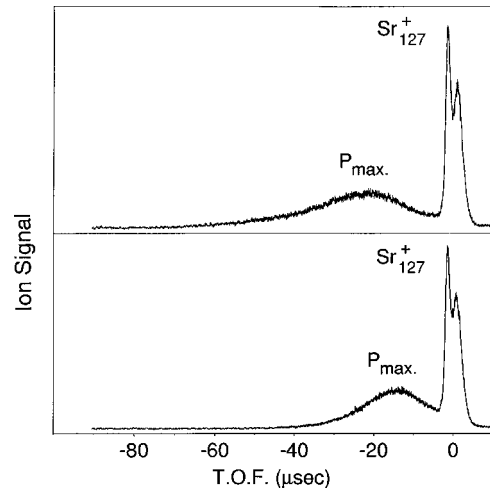


FIG. 2. Photodissociation spectra of the  $\text{Sr}_{127}^+$  parent cluster. The depletion hole in the parent ion peak results from the loss of photoexcited clusters, which evaporate sequentially  $p$  monomers and give rise to the broad pseudo-Gaussian fragment distribution.  $P_{\max}$  is the number of monomers lost at the maximum intensity of the distribution. The excitation photon energy is  $h\nu_{\text{excit}} = 3.50$  eV; the laser fluence is  $87$  mW/cm<sup>2</sup> for the upper trace and  $48$  mW/cm<sup>2</sup> for the lower trace. The origin of the relative time scale is the parent cluster time of flight.

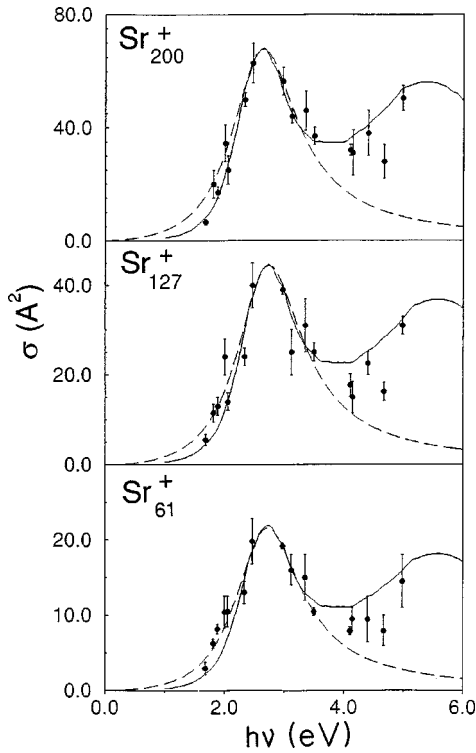


FIG. 3. Cross section profiles for the size  $n=61$ , 127, and 200. Continuous line: fit from Eq. (4) taking the bulk dielectric function (cf. curve of Fig. 4) and including an energy scaling factor  $\times 0.8$ . Dashed line free-electron contribution, Eq. (2).

$$\begin{aligned} \sigma(\omega) &= \frac{4\pi\omega}{c} R^3 \operatorname{Im} \left( \frac{\epsilon(\omega) - 1}{\epsilon(\omega) + 2} \right) \\ &= \frac{24\pi^2 R^3}{\lambda} \frac{\epsilon_2(\omega)}{[\epsilon_1(\omega) + 2]^2 + \epsilon_2^2}, \end{aligned} \quad (4)$$

where  $\epsilon_1(\omega)$  and  $\epsilon_2(\omega)$  are the real and imaginary parts of the bulk dielectric function. From reflectometry measurements described in Ref. 10 one obtains the absorption cross section profile of a “macroscopic” metallic sphere (Fig. 4). It presents two peaks. The dominant one, peaking at 3.4 eV, is associated with the collective excitation of valence electrons. The structure peaking around 7 eV has been interpreted as interband transitions, implying strong  $d$  electron effects.<sup>10</sup> In the same figure the measured absorption cross section of colloidal metallic spherical particles of strontium having dimensions typically in the 3–20 nm range (i.e., 2000 to  $10^6$  atoms), described in Ref. 17, is represented by the long-dashed line, as well as our measurements for  $\text{Sr}_{61}^+$ . The two arrows mark the positions of the  $5s^2(1S_0) \rightarrow 5s5p(1P_1)$  resonance line of Sr,<sup>18</sup> and of the corresponding  $A^1\Sigma_u^+ \rightarrow X^1\Sigma_g^+$  transition of  $\text{Sr}_2$ ,<sup>19</sup> which should develop the collective excitation of  $s$  electrons as cluster size increases. It has to be noted that the absorption cross section of large particles<sup>15</sup> closely approaches the profile of a “macroscopic” strontium sphere, whereas the central part of the absorption profile of  $\text{Sr}_{61}^+$  peaks near the resonance line of Sr.

What is probably the most interesting aspect is the striking similarity between the profile deduced from bulk optical

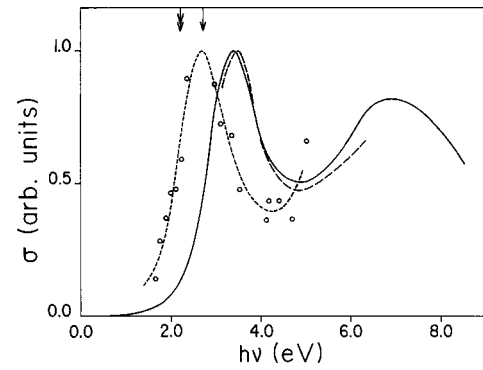


FIG. 4. Continuous line: cross section profile of a macroscopic sphere having the dielectric constant of the bulk. Short-dashed line: experimental cross section profile for  $\text{Sr}_{61}^+$  (guide to the eye from measurement data, open circles). Long-dashed line: cross section profile for spherical metallic particles of strontium in vacuo (after Ref. 17). The profiles are normalized at their maximum value. Vertical arrows indicate the resonance transitions of Sr (right) and  $\text{Sr}_2$  (left).

constants and those observed for clusters. It is remarkable that they can be superimposed provided only that a scaling energy factor is applied (Fig. 3, continuous curves). The best agreement, i.e., the minimum of the standard deviation, is obtained by setting this fitting parameter to the value  $0.8 \pm 0.2$ . This leads to  $\hbar\omega_0 = 2.7 \pm 0.1$  eV for the free-electron part of the profile, a value already obtained by a direct fitting with Eq. (2). The experimental value of  $\sigma^{\text{abs}}$ , normalized to the valence electron number, is comparable to that obtained for the “macroscopic” sphere. It has been mentioned in Ref. 10 that there is a correlation between the optical constant of materials sharing a common crystal structure. So the use of bulk values for  $\epsilon(\omega)$  and of a spherical symmetry in Eq. (4) raises the question of the role of the crystal structure in the  $\sigma(\omega)$  profile. Actually, under our experimental conditions, strontium clusters are hot and in a molten phase.<sup>20</sup> For such floppy objects the atomic structure is compact, close to a sphere, whatever is the crystal structure of the corresponding bulk material. It is reasonable to conclude that the correspondence between experimental  $\sigma(\omega)$  profiles and those deduced from Eq. (4) disentangle the role of electrons, especially in the higher-energy domain of Fig. 3, from that of the shape or crystal structure. Moreover, this correspondence indicates also that a “nonmetal-to-metal transition” is achieved for strontium clusters having more than 61 atoms and that hybridization between  $s$ ,  $p$ , and  $d$  states<sup>21</sup> is already present for such small sizes. Although the phenomenologic scaling factor cannot be explained yet, one must keep in mind that a redshift in the observed resonance frequency for alkali atom clusters has been attributed to electron-ion interaction and to a size-dependent spill-out effect.<sup>14</sup> In the case of the alkaline-earth clusters, these contributions may play a role. Since both the collective excitation and interband transition are shifted as a whole, these two effects are strongly correlated.

In conclusion, the results reported here show that strontium clusters with only sixty atoms present optical properties very similar to those of the bulk material. These similarities

to bulk properties are present not only for collective excitation but also through the interband contribution to the absorption spectrum profiles. More extended measurements toward small sizes should determine the domain of size where

a metal-to-nonmetal transition is expected to occur. These measurements are possible using another experimental method based on the laser fluence dependence of the first evaporated ion peak fragment.<sup>22</sup>

---

\*Permanent address: Institute for Chemical Research, Kyoto University Uji, Kyoto 611-0011, Japan.

<sup>1</sup>G. Gerber, R. Möller, and H. Schneider, *J. Chem. Phys.* **81**, 1538 (1984).

<sup>2</sup>H. Haberland, B. von Issendorf, J. Yufeng, and T. Kolar, *Phys. Rev. Lett.* **69**, 3212 (1992).

<sup>3</sup>K. Rademann, B. Kaiser, U. Even, and F. Hensel, *Phys. Rev. Lett.* **59**, 2319 (1987).

<sup>4</sup>B. Kaiser and K. Rademann, *Phys. Rev. Lett.* **69**, 3204 (1992).

<sup>5</sup>See, e.g., W. A. de Heer, *Rev. Mod. Phys.* **65**, 611 (1993), and references therein; *Clusters of Atoms and Molecules, I*, edited by H. Haberland, Springer Series in Chemical Physics Vol. 52 (Springer, Berlin, 1994).

<sup>6</sup>T. P. Martin, *Phys. Rep.* **273**, 199 (1996).

<sup>7</sup>T. Qureshi and V. Kumar (unpublished).

<sup>8</sup>J. E. Hearn and R. L. Johnston, *J. Chem. Phys.* **107**, 4674 (1997).

<sup>9</sup>C. Bréchnignac, Ph. Cahuzac, J. Leygnier, and A. Sarfati, *Phys. Rev. Lett.* **70**, 2036 (1993).

<sup>10</sup>J. G. Endriz and W. E. Spicer, *Phys. Rev. B* **2**, 1466 (1970).

<sup>11</sup>D. Rayane, P. Mélinon, B. Cabaud, A. Hoareau, B. Tribollet, and

M. Broyer, *Phys. Rev. A* **39**, 6056 (1989).

<sup>12</sup>C. Bréchnignac, Ph. Cahuzac, F. Carlier, and J. Ph. Roux, *Z. Phys.* **28**, 67 (1993).

<sup>13</sup>N. Kébaïli, Ph.D. thesis, 5110, Université Paris-Sud, Centre d'Orsay, 1997.

<sup>14</sup>See, e.g., C. Bréchnignac and Ph. Cahuzac, *Comments At. Mol. Phys.* **31**, 215 (1995).

<sup>15</sup>C. Bréchnignac and J. P. Connerade, *J. Phys. B* **27**, 3795 (1994).

<sup>16</sup>G. Mie, *Ann. Phys. (Leipzig)* **25**, 377 (1908).

<sup>17</sup>J. A. Creighton and D. G. Eadon, *J. Chem. Soc., Faraday Trans.* **87**, 3881 (1991).

<sup>18</sup>C. E. Moore, *Atomic Energy Levels II*, Natl. Bur. Stand. (U.S.) Circ. No. 467 (U.S. GPO, Washington, D.C., 1952).

<sup>19</sup>Ph. Dugourd, J. Chevalyere, C. Bordas, and M. Broyer, *Chem. Phys. Lett.* **193**, 539 (1992).

<sup>20</sup>C. Bréchnignac, Ph. Cahuzac, N. Kébaïli, and J. Leygnier, *Phys. Rev. Lett.* **81**, 4612 (1998).

<sup>21</sup>Y. Kubo, *J. Phys. F* **17**, 383 (1987).

<sup>22</sup>C. Bréchnignac, Ph. Cahuzac, F. Carlier, M. de Frutos, and J. Leygnier, *Chem. Phys. Lett.* **189**, 28 (1992).